

12. I. S. Peschanskii, Ice Sciences and Ice Technology [in Russian], Morskoi Transport, Leningrad (1963).
13. J. M. Dumore et al., "Heat transfer from water to ice by thermal convection," Nature, 172, No. 4375, 460-461 (1953).

EXPERIMENTAL STUDY OF EVAPORATIVE COOLING IN RODS

MADE OF CAPILLARY-POROUS NICHROME

Yu. D. Kolpakov, V. G. Pastukhov,
and V. P. Skripov

UDC 532.685:536.248.2

Results are presented from an experimental study of evaporative liquid cooling in rods of capillary-porous Nichrome with a different structural characteristics in the case of a volumetric heat release ranging from $2 \cdot 10^7$ to $4 \cdot 10^8$ W/m³.

The high efficiency and high rate of heat transfer in systems with evaporative cooling explain the considerable scientific and practical interest in such systems. Experimental results are particularly important for constructing a proper physical model of the evaporation of a liquid in capillary-porous materials. Published works on the porous cooling of materials with volumetric heat release do not contain any data on such systems in the case where evaporation occurs through the lateral surface of a porous cylindrical specimen in which capillary makeup was accomplished through the ends. There has also been no study of the cooling of a previously impregnated specimen without makeup. Such a system differs significantly from conventional systems [1, 2], in which coolant is pumped through a porous layer and evaporation occurs at the opposing surface.

The goal of the present experimental study is to investigate liquid evaporation from porous cylindrical Nichrome rods in relation to the structural characteristics, the energy supplied, and the conditions of delivery of the liquid being evaporated. The formulation of the problem and the experiment is dictated by the problem of determining the limiting values of volumetric heat release in a porous material with a continuous makeup of the evaporating liquid as a result of capillary forces. Such information can be of practical value in several instances involving heat transfer in capillary-porous materials.

The method of powder metallurgy was used to make porous cylindrical specimens 8 mm in diameter and 80 mm in length (Table 1). The porosity of the finished specimens was determined by the gravimetric method. Maximum pore size was determined by the method of displacing liquid from an impregnated specimen.

Evaporative cooling was studied on the experimental unit shown in Fig. 1.

TABLE 1. Characteristics of Capillary-Porous Structures of Nichrome (80% Ni, 20% Cr)

Number of group	Fraction of original powder, μm	Porosity, %	Maximum pore radius, μm
1	0—40	52	6
2	40—75	60	12
3	75—125	64	20

Department of Physicotechnical Problems of Power Engineering, Ural Science Center, Academy of Sciences of the USSR, Sverdlovsk. Translated from Inzhenerno-Fizicheskii Zhurnal, Vol. 48, No. 4, pp. 617-621, April, 1985. Original article submitted March 26, 1984.

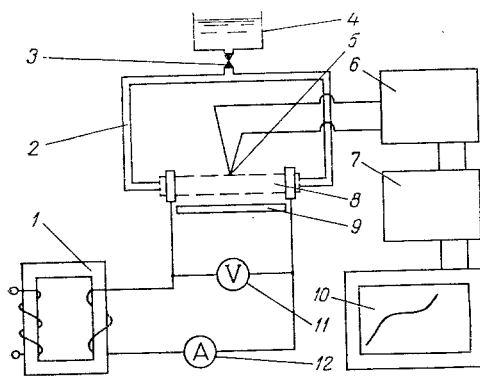


Fig. 1

Fig. 1. Block diagram of the experimental unit: 1) TDM-3192 welding transformer; 2) pipe for delivering liquid; 3) valve; 4) measuring vessel with liquid; 5) thermocouple junction; 6) R37/1 direct-current potentiometer; 7) F116/1 microvolt-ammeter; 8) specimen; 9) base for collecting liquid not participating in evaporation; 10) KSP-4 automatic potentiometer; 11) V7-20 digital voltmeter; 12) ammeter with UTT-5 current transformer.

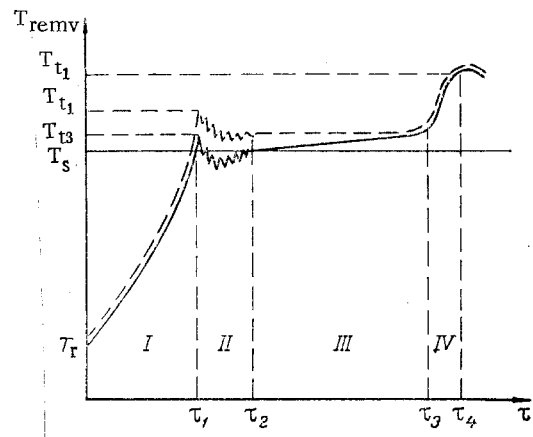


Fig. 2

Fig. 2. Thermogram of liquid evaporation from a porous material: for group 1 specimens (dashed lines) and for group 3 specimens (solid lines).

Volumetric heat release in a capillary-porous material was accomplished by passing an alternating current of from 60 to 400 A through the material. Unit volumetric heat release q_V was calculated from the energy liberated in the specimen. In the experiment we realized the range $q_V = (2-40) \cdot 10^7 \text{ W/m}^3$. We used distilled water as the filler. The porous specimens were impregnated by boiling in water before each test and subsequently cooling them. A copper-constantan thermocouple with diameter 0.12 mm was soldered to the specimen surface to measure temperature. The thermocouples were installed in the center of the surface of the working section since intensive evaporation and the maximum increase in temperature occur here in the case of drying of the specimen. The latter occur because, along with convective heat exchange with the environment and cooling due to evaporation, heat is removed in the massive current conductors. The temperature of the conductors during the tests remained nearly equal to the room temperature. The emf from the thermocouple was recorded by a potentiometer, which made it possible to monitor the change in the temperature of the surface over time. In each test we weighed the specimens and base before and after evaporation to determine the amount of liquid that evaporated and the amount lost due to its thermal expansion and ejection during boiling.

The unit was used to conduct two series of tests: the first series involved study of evaporative cooling on specimens previously impregnated with water in which the water was not made up; the second series used specimens in which the water was made up through the ends of the specimens. Study of evaporation in the former specimens (no makeup) allowed us to construct a physical picture of the phenomena observed.

The evaporation of a liquid in cylindrical specimens in the case of volumetric heat release can be tentatively divided into four regions characterized by different thermal regimes (Fig. 2). In region I, from the moment of application of the load to the time τ_1 , specimen temperature increases from room temperature to the boiling point on the saturation line $T_S = 100^\circ\text{C}$. During this time liquid is displaced as a result of an increase in its volume with the increase in temperature, with some of the liquid remaining on the surface in the form of drops. Region II is characterized by intensive boiling of the water on the surface and its partial spraying. We should note the presence of a certain amount of superheating at the beginning of the second region. The amount of superheating T_{h1} is greater on the specimens with small pores (group 1) than on the large-pore specimens (group 3) (see Table 1). This increase in temperature is attributable to the need for superheating to increase the vapor pressure in the bubbles by an amount corresponding to the capillary pressure [$2\sigma/r_m = (0.6-2) \cdot 10^4 \text{ N/m}^2$]. It can be suggested that the boiling point also increases due to the pressure

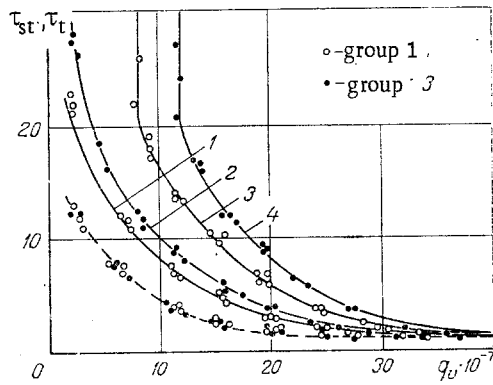


Fig. 3. The function $\tau_t(q_v)$ for all specimens with makeup and without makeup (dashed line) and $\tau_{st}(q_v)$ (solid lines): 1) for group 1 specimens without makeup; 2) for group 3 specimens without makeup; 3) for group 1 specimens with makeup; 4) for group 3 specimens with makeup. q_v , W/m^2 ; τ_t , τ_{st} , sec.

increase in the pores of the capillary-porous material resulting from thermal expansion of the liquid. This is supported by the empirically established dependence of the amount of superheating on the heat release. At $q_v = 35 \cdot 10^7$ W/m^2 , superheating reached $5^\circ C$ on the group 1 specimens and $3^\circ C$ on the group 3 specimens. The amount of superheating decreases with time. By the time τ_2 the temperature fluctuations have ceased, the evaporation region has extended deeper into the material, and a stable boiling regime has begun (region III). The temperature of the surface of a large-pore specimen becomes equal to T_s , and as the evaporation region extends deeper into the material the temperature in the pores increases uniformly. Here, along with diffusion resistance to the vapor flow, there arises viscous drag. The pressure above the meniscus increases and the boiling point is shifted toward higher temperatures. The same result was found in [3].

In the case of specimens with small pores, during the entire third stage of boiling there is constant superheating. This superheating continues until complete evaporation of the liquid in the central part of the specimen. From the moment τ_3 that evaporation is completed, the specimen dries up and temperature increases sharply. When the temperature of $110^\circ C$ was reached at a certain moment of time τ_4 , the load was automatically removed to prevent severe overheating. The specimen was then cooled by convection with the environment.

Analysis of thermograms also made it possible to determine the dependence of the transitional τ_t and quasisteady τ_{st} regimes on the heat release for Nichrome specimens with different structural characteristics (Fig. 3), where $\tau_t = \tau_1$ and $\tau_{st} = \tau_3 - \tau_1$.

In the calculations we used the heat balance equation without allowance for the loss in heating of the current conductors, convective heat exchange with the environment, and radiation:

$$UI(\tau_s + \tau_{st}) = (c_w m_w + c_c m_c) \Delta T + I_w (m_w - m_{los}).$$

It is apparent from the figure that, given the same geometric dimensions and different porosities, the duration of the transitional regime is basically independent of the structural characteristics of the materials. This is because, on the whole, it is determined by the heat capacity of the system, and practically the same relation $\tau_t(q_v)$ is obtained in the porosity range 52-64%. The noncoincidence of the curves of $\tau_{st}(q_v)$ for the specimens of groups 1 and 3 is due to the difference in porosity, and because of the different amounts of liquid evaporated the durations of the steady-state regime will be different. In tests with makeup of the coolant it is important to determine the limiting thermal loads. When these loads are exceeded, the capillary makeup is disrupted and the steady boiling regime is disturbed. The limiting heat release was $8 \cdot 10^7$ in the small-pore structures (group 1), while it was $12 \cdot 10^7$ W/m^2 in the large-pore structures (group 3). This is reflected by curves 3 and 4 (Fig. 3). The above limiting heat fluxes were determined with a balance between evaporation and the supply of liquid. The rate of liquid delivery with capillary makeup is a constant for a specific liquid-capillary-body system and is characterized by a constant rate of capillary makeup [4]. It is proportional to the pore size. Taking this into consideration, we see that the main factor determining the limiting heat release in a steady regime with makeup for a given system is pore size.

In the tests with makeup we observed a pulsative change in specimen surface temperature, which is evidence of periodic saturation of the specimen by liquid with subsequent drying.

Taking the above into consideration with regard to the mechanism of evaporation in the tests without makeup, these pulsations can be explained as follows. The movement of the evaporation region deeper into the specimen causes an increase in pressure inside the porous material. This prevents liquid from flowing to the surface under the influence of capillary forces. When evaporation is completed, pressure falls, and in the case $q_v < q_{vlim}$ makeup of the liquid begins anew and the cycle is repeated.

An evaluation of the liquid consumption showed that the amount of water lost as a result of volumetric expansion and entrainment by the vapor flow is on the order of 40%. Thus, 60% of the water is expended in evaporation. Unfortunately, the low accuracy of the coolant consumption determination, connected with the difficulty of collecting the liquid drops carried off by the vapor, made it impossible to make a quantitative conclusion regarding the effect of pore size on the magnitude of the unproductive losses of liquid. However, it can be asserted that an increase in pore size is accompanied by an increase in liquid loss.

NOTATION

τ , time, sec; T , temperature, °C; U , voltage drop over the specimen, V; I , current, A; c_w , c_c , specific heats of water and Nichrome, J/kg·K; m_w and m_c , weight of water in the specimen and weight of the dry specimen, kg; m_{los} , weight of the water not participating in evaporation, kg; L_w , heat of vaporization of water, J/kg; q_v , heat release, W/m²; σ , surface tension, N/m; r_m , maximum pore radius, m; T_r , room temperature; T_s , saturation temperature; T_{h1} , superheating temperature on the group 1 specimens; T_{h3} , heating temperature on the group 3 specimens; T_{remv} , temperature at which the load is removed; τ_1 , time required to reach T_s ; τ_2 , beginning of extension of evaporation into the body of the specimen; τ_3 , completion of evaporation in the central part of the specimen; τ_4 , moment of load removal.

LITERATURE CITED

1. V. A. Maiorov and L. L. Vasil'ev, "Heat transfer and stability in the motion of a coolant evaporating in porous metal-ceramic materials," *Inzh.-Fiz. Zh.*, 20, No. 5, 965-970 (1979).
2. V. A. Maiorov and L. L. Vasil'ev, "Structure of an evaporating flow inside a heated porous material," *Inzh.-Fiz. Zh.*, 41, No. 6, 914-935 (1981).
3. V. B. Lisovskii, "Experimental study of heat and mass transfer in the evaporation of nitrogen from a capillary-porous body," in: *Energy and Mass Transfer Processes in Porous Media with Phase Transitions [in Russian]*, ITMO Akad. Nauk BSSR (1982), pp. 71-76.
4. B. A. Borok and I. N. Golikov, "Study of the kinetics of impregnation of porous metal-ceramic bodies," *Fiz. Khim. Obrab. Mater.*, No. 2, 101-110 (1968).